Lone interactions involving an aromatic -system : cComplexes of hexafluorobenzene with dimethyl ether and trimethylamine

Lone pair···π interactions involving an aromatic π-system: Complexes of hexafluorobenzene with dimethyl ether and trimethylamine.

Yannick Geboes[a,b], Frank De Proft[b] and Wouter A. Herrebout[a]*

[a] *Department of Chemistry, University of Antwerp, Groenenborgerlaan 171, 2020 Antwerp (Belgium), E-mail: Wouter.herrebout@uantwerpen.be*
[b] *Eenheid Algemene Chemie (ALGC), Member of the QCMM VUB-UGent Alliance Research Group, Vrije Universiteit Brussel (VUB), Pleinlaan 2, 1050 Brussels (Belgium)*

Corresponding Author:

W.A. Herrebout: e-mail: wouter.herrebout@uantwerpen.be, +32/3.265.33.73

Keywords: lp···π interactions, hexafluorobenzene, FTIR, cryospectroscopy

Abstract

The formation of complexes between hexafluorobenzene and the Lewis bases dimethyl ether, dimethyl ether-d_6, trimethylamine and trimethylamine-d_9 was investigated experimentally using FTIR spectroscopy on solutions of liquid krypton. Additional bands found in the spectra of mixtures were assigned to lone pair···π complexes using *ab initio* calculations at the MP2/aug-cc-pVDZ level. By constructing Van 't Hoff plots, experimental complexation enthalpies were determined of -6.0(6) kJ mol^{-1} for the complex with dimethyl ether(-d_6) and -6.7(9) kJ mol^{-1} for the complex with trimethylamine(-d_9). These values are in good agreement with calculated enthalpy values.

Introduction

The electrostatic potential on the molecular surface of unsaturated, locally electron deficient molecules shows a region of positive electrostatic potential, perpendicular to (a part of) the molecular framework, often denoted as a π-hole. [1] In recent years it has been shown both theoretically [2-3] and experimentally [4-5] that molecules are able to form noncovalent interactions with anions and lone pairs of Lewis bases through this π-hole, forming anion···π and lone pair···π (lp···π) complexes, respectively. A review concerning these noncovalent interactions has recently been published by Bauzá et al. [6]

The most studied lp···π complex is undoubtedly the hexafluorobenzene-water (C_6F_6–H_2O) complex, which has been described in much detail both theoretically [7-8] and experimentally. [9-13] The interest in C_6F_6 can be attributed to its use as a solvent in several spectroscopic techniques as well as its use as a

standard in ^{19}F NMR and ^{13}C NMR. Furthermore, C_6F_6 acts as a good model compound for perfluorinated aromatic rings in larger organic compounds, such as perfluorohalocarbons (PFHC's), which are often used in the fields of crystal engineering and supramolecular chemistry.[14-15] Therefore, a good understanding of the nature of the interactions with these compounds is crucial. Furthermore, as halogen atoms are often used to withdraw electrons from the π-system, lp···π interactions are often found in systems where halogen bonds are also present. To illustrate the influence of halogenation on the π-system, the electrostatic potential on the molecular surfaces of benzene and C_6F_6 are shown in Figure S1.

It should be noted however that the formation of lp···π complexes is not limited to aromatic bond donors, such as C_6F_6, but can also be found for non-aromatic donors containing an electron deficient π-system, such as the C_2F_3X (X=F, Cl, Br, I) systems. The existence of lp···π bonded complex at thermodynamic equilibrium between the donor molecules C_2F_4 and C_2F_3Cl and Lewis bases dimethyl ether [16] and trimethylamine [17] has already been demonstrated. Furthermore, lp···π complex was also found experimentally using pulsed-jet Fourier transform microwave spectroscopy for the complexes of C_2F_3Cl with water, [18] dimethyl ether and ammonia. [19]

Even though the complexes between C_6F_6 and different Lewis bases have been described theoretically, [20-21] experimental results supporting these findings, apart from the complex formed with water, are still scarce. [22] In this study the complexes between C_6F_6 and dimethyl ether (DME) and trimethylamine (TMA) have been evaluated at equilibrium conditions using FTIR spectroscopy of liquid noble gas solutions.

Experimental and Computational methods

Hexafluorobenzene (C_6F_6) was purchased from Sigma-Aldrich and had a stated purity of +99.5%. The sample was transferred into a sample tube and degassed using the freeze-thaw cycle procedure. Dimethyl ether (99+%), dimethyl ether-d_6 (98+% d), trimethylamine (99%) and trimethylamine-d_9 (+99% d) were also purchased from Aldrich and were used without further purification steps. The solvent gas krypton was supplied by Air Liquide and had a stated purity of 99.9995%.

The infrared spectra were recorded on a Bruker 66v FTIR spectrometer, equipped with a globar source, a Ge/KBr beam splitter and MCT detector, cooled with liquid nitrogen. All interferograms were averaged over 500 scans, Blackman-Harris 3-term apodized and Fourier transformed with a zero filling factor of 8 to yield spectra with a resolution of 0.5 cm^{-1}. Thermal expansion of the solvent gas during temperature studies was accounted for using the method published by van der Veken. [23] The numbering of the fundamental vibrational modes of DME, DME-d_6, TMA, TMA-d_9 and C_6F_6 follows the numbering scheme of Herzberg. [24-25] To aid assignments and avoid spectral congestion, measurements are performed using both undeuterated and fully deuterated Lewis bases. When

referring to (measurements or results of) both the undeuterated and fully deuterated Lewis bases, the notations DME(-d_6) and TMA(-d_9) are used in the remainder of this paper, whereas the parentheses are omitted when referring to the deuterated species only. As the experimental setup does not allow for verification of full solubility of the compounds, exact concentrations are not known. Estimated mole fractions of the solutions varied between 1.9×10^{-5} and 1.9×10^{-2} for C_6F_6, 6.6×10^{-4} and 2.8×10^{-2} for DME(-d_6) and 5.6×10^{-4} and 1.5×10^{-2} for TMA(-d_9). In order to obtain spectra in which the bands of interest have a maximal absorbance of 1, combined with the necessity to retain an appreciable amount of complex, solutions containing a limited amount of the molecule of interest with a large excess of the other molecule were prepared.

To support the experimental measurements, *ab initio* MP2 calculations were performed using Dunning's augmented correlation consistent basis sets of double zeta quality (aug-cc-pVDZ) in Gaussian09. [26] The counterpoise technique as proposed by Boys and Bernardi was used during all *ab initio* calculations to account for the basis set superposition error. [27] Energies at the basis set limit were calculated with Molpro [28] using the extrapolation scheme of Truhlar, in which the effect of electron correlation is obtained from MP2 calculations. [29]

$$E_{CBS}^{HF} = \frac{3^{\alpha}}{3^{\alpha} - 2^{\alpha}} E_3^{HF} - \frac{2^{\alpha}}{3^{\alpha} - 2^{\alpha}} E_2^{HF} \quad (1)$$

$$E_{CBS}^{cor,MP2} = \frac{3^{\beta}}{3^{\beta} - 2^{\beta}} E_3^{cor,MP2} - \frac{2^{\beta}}{3^{\beta} - 2^{\beta}} E_2^{cor,MP2} \quad (2)$$

In these calculations $\alpha = 3.4$ and $\beta=2.2$, [29] while energies with subscript 2 and 3 are calculated using the aug-cc-pVDZ and aug-cc-pVTZ basis sets respectively.

Furthermore, a correction for higher order correlation effects is made using Hobza's method, [30] yielding results of $E_{CBS}^{CCSD(T)}$ quality.

$$\Delta E^{CCSD(T)} = \left| E^{CCSD(T)} - E^{MP2} \right|_{aug-cc-pVDZ(-PP)} \quad (3)$$

$$E_{CBS}^{CCSD(T)} = E_{CBS}^{HF} + E_{CBS}^{cor,MP2} + \Delta E^{CCSD(T)} \quad (4)$$

Complexation enthalpies in the gas phase ΔH°(vap,calc) were obtained from the calculated complexation energies ΔE(CCSD(T)) by applying a zero-point energy correction and a correction for thermal effects, obtained from statistical thermodynamics at MP2/aug-cc-pVDZ level of theory, calculated at 138 K, the center of the experimental temperature interval of 120 K to 156 K. By correcting these calculated enthalpy values with solvent effects, obtained from the Monte Carlo Free Energy Perturbation (MC-FEP) approach using an in-house modified version of BOSS 4.0 [31], complexation enthalpies in solution ΔH°(LNg,calc) are obtained which can be compared with the experimental complexation enthalpies ΔH°(LNg). A full description of the computation methods used has been summarized before. [32]

Results and discussion:

From the *ab initio* MP2/aug-cc-pVDZ calculations, only one stable complex isomer was found for both Lewis bases, in which the lone pair of the Lewis base faces the center of the C_6F_6 ring. The MP2/aug-cc-pVDZ optimized structures of both complexes are given in Figure 1, whereas intermolecular parameters of the complexes as well as calculated complexation energies and calculated and experimental complexation enthalpies are given in Table 1. Cartesian coordinates of the monomer and complex geometries are given in Tables S1 and S2 of the ESI.

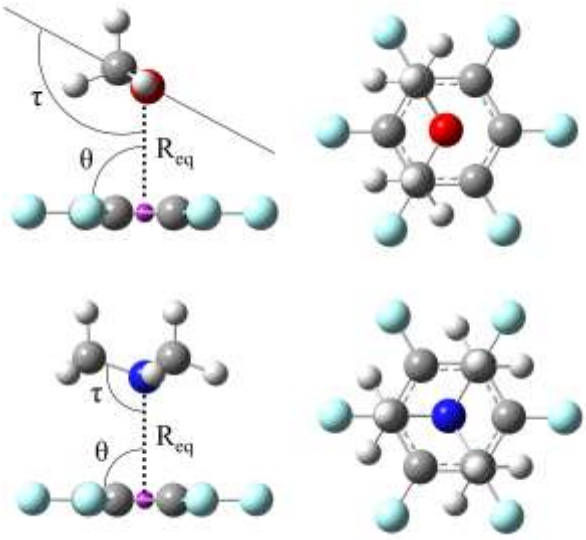

Figure 1: MP2/aug-cc-pVDZ equilibrium geometries for the O···π complex between C_6F_6 and DME (top) and N···π complex between C_6F_6 and TMA (bottom), including the designation of the binding distance and angles given in Table 1. The centroid of the C_6F_6 ring is shown in purple.

Table 1: Intermolecular distance R_{eq} (Å) between the donor atom and the centroid of the C_6F_6 ring, bond angles and dihedrals (°), calculated complexation energies at different levels of theory and experimental complexation enthalpies (kJ mol^{-1}) for the complexes of C_6F_6 with DME and TMA.

lp···π bonded	C_6F_6·DME	C_6F_6·TMA
Symmetry	C_s	C_{3v}
$R_{eq}=R_{\pi\cdots Y}$	2.99	3.02
θ	91.04	90.05/89.95
τ	121.64	108.86
ΔE (DZ) [a]	-19.8	-25.8
ΔE (TZ) [b]	-21.2	-27.2
ΔE (CCSD(T)) [c]	-19.6	-24.3
Δ*H*° (vap,calc)	-17.4	-22.4
Δ*H*° (LKr,calc)	-7.8	-9.3
Experimental [d]		
Δ*H*° (LKr)	-6.0(6)	-6.7(9)

[a] MP2/aug-cc-pVDZ energy, [b] MP2/aug-cc-pVTZ energy, [c] CCSD(T)/CBS extrapolated energy, [d] values determined in the 120 K – 156 K temperature interval.

From the complex geometry shown in Figure 1 and the geometrical parameters in Table 1 it can be clearly seen that the lone pair of oxygen faces towards the π-system of C_6F_6, resulting in a lp···π interaction formed through the center of the ring, the angle θ between the oxygen-centroid line and the molecular plane of C_6F_6 being 91.04°. The angle between the DME bisector and the oxygen-centroid line (τ) of 121.64° shows that the dimethyl ether molecule is tilted towards the C_6F_6 molecular plane and is also consistent with the rabbit-ear configuration of the lone pairs on the oxygen atom. This tilted position also enables the formation of secondary interactions between the methyl groups of DME and C_6F_6. In order to visualize these secondary interactions, the lp···π complexes were analyzed using the noncovalent interactions index visualized using NCIPLOT [33-34], for which the results are given in Figure S2 of the ESI. In Figure S2, the presence of interaction surfaces between the methyl groups and C_6F_6 can be seen, adjoined to the bowl-like surface caused by the O···π interaction. Optimization of this complex with and without imposing C_s symmetry yielded the same complexation geometry and energy. Rotation of DME above the C_6F_6 molecular plane yields a transition state with an increase in energy of 0.12 kJ mol^{-1} compared to the ground state. For this transition state, a single imaginary frequency was found of 10.9*i* cm^{-1}. As this energy barrier is smaller than the kT value at 120 K, the existence of large amplitude motions is expected.

For the complex between C_6F_6 and TMA, shown in Figure 1, a complex geometry with C_{3v} symmetry, in which the lone pair of the Lewis base faces directly to the centroid of the C_6F_6 ring is observed, the angle between the nitrogen atom, C_6F_6 centroid and C_6F_6 carbon atom (θ) being either 90.05° or 89.95° for carbon atoms of the C_6F_6 ring which are eclipsed and non-eclipsed with the TMA carbon atoms, respectively. Optimization without symmetry restrictions yielded the same complex geometry. Apart from the bowl-like surface caused by the N···π interaction, only very small secondary interaction surfaces between the methyl groups and C_6F_6 are observed for this complex in the gradient isosurfaces shown in Figure S2. The complex geometry in which C_6F_6 and TMA have been rotated 60° from each other, leading to a staggered configuration with C_{3v} symmetry, increased the energy by 0.09 kJ mol^{-1} and yielded one imaginary frequency (8.6*i* cm^{-1}). Also here the existence of large amplitude motions is expected.

When comparing the complexation energies of both complexes, a decrease in complexation energy of 0.2 kJ mol^{-1} and 1.5 kJ mol^{-1} for the complexes with DME and TMA respectively can be observed when going from the MP2/aug-cc-pVDZ level to the (extrapolated) CCSD(T)/CBS level. Upon correction of the CCSD(T)/CBS energies for zero-point energy, thermal and solvent effects to obtain complex enthalpies Δ*H*°(LKr,calc), the complex with TMA remains stronger than the complex with DME, the difference in strength between both complexes, however, diminishes from -4.7 to -1.6 kJ mol^{-1}.

In order to determine the nature of the attractive interaction, an NBO analysis of both complexes was performed. However, as in a previous study [17], this analysis did not yield clear results as to which electron transfers are responsible for the attractive interaction. It was found that the charge transfer for both complexes is smaller than 0.001, which indicates that the attraction is mainly electrostatic, rather than due to charge transfer.

Experimental assignment of the vibrational modes of the Lewis bases is based on assignments of liquefied noble gas solutions found in the literature. [35-37] To aid the assignment of the DME-d_6 modes, the anharmonic force field of DME-d_6 was also calculated using Gaussian09 at the MP2/aug-cc-pVDZ level. For the assignment of C_6F_6, gas phase [38-39] and matrix isolation frequencies[10] found in the literature were used.

From the *ab initio* calculated frequencies, given in Tables S4 to S7 of the ESI, it is clear that only 4 out of 20 vibrational modes are IR active, of which ν_4 and ν_{14} lie outside the studied spectral range. The remaining vibrational modes ν_{12} and ν_{13} have a large IR intensity, resulting in the use of diluted solutions for the study of these vibrational modes. Apart from these fundamental transitions, two further bands at 1024.8 cm^{-1} and 1016.9 cm^{-1} are observed in these solutions, which are the result of a complex Fermi resonance in this spectral range and have been described before in the gas phase. Possible assignments are the double combination $\nu_{11} + \nu_{19}$, the triple combination $\nu_{14} + \nu_{17} + \nu_{18}$ and the quadruple combinations $\nu_8 + 2\nu_{14} + \nu_{20}$, $\nu_{10} + \nu_{11} + \nu_{14} + \nu_{20}$ and $\nu_{14} + \nu_{17} + 2\nu_{20}$. It should also be noted that the relative intensity of the bands in this spectral region differs strongly with those observed previously in a solid N_2 matrix, where the band at 1016.9 cm^{-1} is not observed, [10] and the low resolution gas phase spectra, in which the band with the highest frequency has the largest intensity. [39] The infrared spectrum of the ν_{12} and ν_{13} spectral region of C_6F_6 for a C_6F_6 solution in LKr is given in Figure S3.

For both observable fundamental bands of C_6F_6, shown in panels A and B of Figure 2, an additional band is observed in the spectra of mixtures of C_6F_6 with DME upon subtraction. For the ν_{12} mode (panel A), a blue shifted band with a shift of 0.9 cm^{-1} is observed, whereas a redshifted band with a shift of -1.2 cm^{-1} appears near the ν_{13} band (panel B). Both complexation shifts are in good agreement with the calculated complexation shifts for the lp$\cdots\pi$ complex of 1.3 cm^{-1} and -2.8 cm^{-1}, respectively. To study complex bands of the DME(-d_6) modes, solutions with increased concentrations of C_6F_6 were measured. A spectrum of the ν_6 spectral region of DME is also shown in Figure 2, panel C, in which a complex band with a -3.9 cm^{-1} redshift, corresponding to the calculated shift of -6.1 cm^{-1} for the lp$\cdots\pi$ complex, can be observed. Spectra of the above mentioned spectral ranges for $C_6F_6\cdot$DME-d_6 mixtures are given in Figure S4 of the ESI. An assignment of the monomers and corresponding complex bands is given in Table 2 for DME and in Table S8 for DME-d_6.

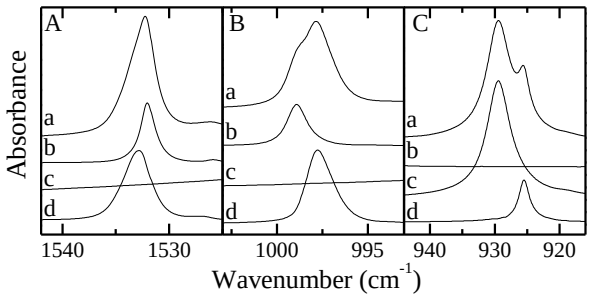

Figure 2: Infrared spectra of the C_6F_6 ν_{12} spectral region (panel A), C_6F_6 ν_{13} spectral region (panel B) and DME ν_6 spectral region (panel C) of solutions of mixtures of C_6F_6 and DME dissolved in LKr at 120 K. In each panel, trace *a* represents the mixed solution, while traces *b* and *c* show the solution containing only C_6F_6 or DME, respectively. Trace *d* represents the spectrum of the complex and is obtained by subtracting the rescaled traces *b* and *c* from trace *a*.

Table 2: Experimental infrared frequencies for the monomer and complex, as well as experimental complexation shifts ($\Delta\nu_{exp}$) and MP2/aug-cc-pVDZ calculated complexation shifts ($\Delta\nu_{calc,O\cdots\pi}$), in cm^{-1}, for the $O\cdots\pi$ bonded complex of C_6F_6 with DME dissolved in LKr at 120 K.

	Assignment	Symmetry	$\nu_{monomer}$	$\nu_{complex}$	$\Delta\nu_{exp}$	$\Delta\nu_{calc,O\cdots\pi}$
C_6F_6	ν_{12}	E_{1u}	1532.0	1532.9	0.9	1.3
	ν_{12} ^{13}C	E_{1u}	1525.9	1527.1	1.2	1.3
			1024.8	1024.9	0.1	
			1016.9	1017.0	0.1	
	ν_{13}	E_{1u}	999.0	997.8	-1.2	-2.8
DME	ν_1	A_1	2990.4	2990.5	0.1	-8.5
	ν_{16}	B_2	2990.4	2990.5	0.1	-8.6
	ν_{12}	B_1	2916.6	2919.5	2.9	1.8
	ν_2	A_1	2811.9	2816.1	4.2	-2.7
	ν_{18}	B_2	1457.7	1458.4	0.7	-0.1
	ν_{13}	B_1	1454.9	1454.7	-0.2	-2.3
	ν_{19}	B_2	1426.3	1425.3	-1.0	-0.7
	ν_5	A_1	1245.1	1245.9	0.8	-2.0
	ν_{20}	B_2	1172.1			-6.9
	ν_{21}	B_2	1099.1			-4.0
	ν_6	A_1	929.4	925.5	-3.9	-6.1

For mixtures of C_6F_6 with TMA($-d_9$), spectra of the fundamental bands of C_6F_6 are given in Figures 3 (TMA) and S5 of the ESI (TMA-d_9). The C_6F_6 ν_{13} spectral region of the mixture with TMA-d_9 is not given due to overlap with the ν_5 mode of TMA-d_9. As with DME, a blue shifted complex band, with a shift of 0.8 cm^{-1} is observed in the ν_{12} spectral region (panel 3A), as well as a -2.5 cm^{-1} redshifted complex band in the ν_{13} region (panel 3B). Both bands are again in good agreement with the calculated values for the $lp\cdots\pi$ complex of 1.3 cm^{-1} and -3.9 cm^{-1}, respectively. An assignment of the monomers and corresponding complex bands is given in Table 3 for TMA and in Table S9 for TMA-d_9.

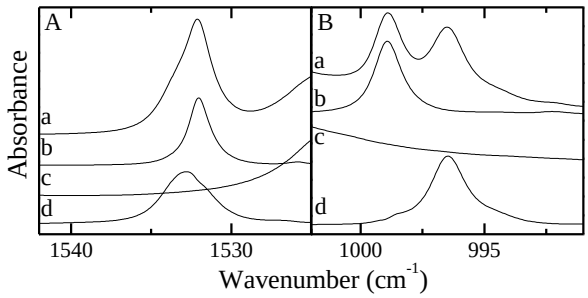

Figure 3: Infrared spectra of the C_6F_6 ν_{12} spectral region (panel A) and C_6F_6 ν_{13} spectral region (panel B) of solutions of mixtures of C_6F_6 and TMA dissolved in LKr at 120 K. In each panel, trace *a* represents the mixed solution, while traces *b* and *c* show the solution containing only C_6F_6 or TMA, respectively. Trace *d* represents the spectrum of the complex and is obtained by subtracting the rescaled traces *b* and *c* from trace *a*.

Table 3: Experimental infrared frequencies for the monomer and complex, as well as experimental complexation shifts ($\Delta\nu_{exp}$) and MP2/aug-cc-pVDZ calculated complexation shifts ($\Delta\nu_{calc,\ N\cdots\pi}$), in cm^{-1}, for the $N\cdots\pi$ bonded complex of C_6F_6 with TMA dissolved in LKr at 120 K.

	Assignment	Symmetry	$\nu_{monomer}$	$\nu_{complex}$	$\Delta\nu_{exp}$	$\Delta\nu_{calc,N\cdots\pi}$
C_6F_6	ν_{12}	E_{1u}	1532.0	1532.8	0.8	1.3
	ν_{12} ^{13}C	E_{1u}	1525.9	1527.1	1.2	1.3
			1024.8	1021.5	-3.3	
			1016.9	1014.4	-2.5	
	ν_{13}	E_{1u}	999.0	996.5	-2.5	-3.9
TMA	ν_{12}	E	2977.0	2978.4	1.4	-11.1
	ν_1	A_1	2944.4	2944.2	-0.2	-9.2
	ν_{13}	E	2944.4	2944.2	-0.2	-9.1
	$2\ \nu_4$	A_1	2818.6	2822.6	4.0	1.4
	ν_2	A_1	2769.0	2773.1	4.1	7.3
	ν_{14}	E	2769.0	2773.1	4.1	8.5
	$\nu_{20}+\nu_{21}$	E	1474.8	1472.8	-2.0	-4.1
	ν_{15}	E	1467.6	1468.7	1.1	1.7
	ν_3	A_1	1454.8	1454.3	-0.5	-3.2
	ν_4	A_1	1438.8	1437.6	-1.2	0.7
	ν_{16}	E	1438.8	1437.6	-1.2	-3.8
	ν_{17}	E	1405.3			0.1
	ν_{18}	E	1273.3	1271.4	-1.9	-2.1
	ν_5	A_1	1184.3	1187.1	2.8	0.9
	ν_{19}	E	1098.5	1098.4	-0.1	-2.2
	ν_{20}	E	1041.5	1039.3	-2.2	-1.8
	ν_6	A_1	828.1	826.5	-1.6	-3.8

Even though calculated and experimental shifts are in good agreement for most vibrational modes, some discrepancies can be found in Tables 2, 3, S8 and S9 regarding the complexation shift direction. Many of the vibrational modes with inconsistent shifts are found in the C-H stretching region (around 3000 cm^{-1} for the undeuterated and 2000 cm^{-1} for the deuterated Lewis bases), where, apart from the fundamentals, many overtones and combination bands are found. Therefore the complexation shifts in

this region are often perturbed by Fermi resonances, and the assignment of these complex bands is rather difficult. For the DME ν_{18} mode both the calculated and experimental shifts are very small, whereas the DME ν_5 mode (CH_3-rocking mode) is very sensitive to the orientation of the DME molecule towards C_6F_6 in the complex, which might be influenced by the small rotational barrier discussed before. For DME-d_6 the vibrational modes ν_{13}, ν_{20} and ν_{19} have a large overlap, so that the spectra had to be decomposed in order to determine frequencies. For TMA the discrepancy for the ν_4 mode can be explained by the overlap with ν_{16} mode, which has a red shift, as calculated.

By constructing Van 't Hoff plots from measurements between 120 K and 156 K, 7 experimental complexation enthalpies between -5.0 and -6.8 kJ mol^{-1} have been determined for the lp$\cdots\pi$ complex of C_6F_6 with DME(-d_6), the average being of -6.0(6) kJ mol^{-1}. For the lp$\cdots\pi$ complex with TMA(-d_9), 5 experimental complexation enthalpies were determined between -5.6 kJ mol^{-1} and -8.1 kJ mol^{-1}, with an average value of -6.7(9) kJ mol^{-1}. An example of a Van 't Hoff plot for each complex is shown in Figure S6 of the ESI. Further detailed information on the subtraction procedure and numerical integration for the Van 't Hoff plots is available upon request.

Apart from the 1:1 complexes described above, 1:2 complexes in which 2 Lewis base molecules form an anti-cooperative sandwich complex on opposite sides of the C_6F_6 molecular plane can be envisaged. Such complexes have been observed experimentally in studies involving benzene and a large excess of the donor molecules CF_3I [40] and halothane [41]. The existence of (an appreciable amount of) 1:2 complex typically results in the formation of complex bands at the lowest temperatures near the C_6F_6 monomer bands with shifts greater than those of the 1:1 complex. Indeed, MP2/aug-cc-pVDZ *ab initio* calculations of the $C_6F_6\cdot$2DME complex with C_{2h} symmetry and $C_6F_6\cdot$2TMA complex with D_{3h} symmetry, for which the Cartesian coordinates are given in tables S3.1 and S3.2 of the ESI confirm that the complexation shifts of the ν_{12} and ν_{13} modes of C_6F_6 are about two times larger than the complexation shift of the 1:1 complexes. Calculation of the vibrational frequencies confirmed that both complex geometries are real minima. Complexation energies at the MP2/aug-cc-pVDZ level are -38.7 kJ mol^{-1} and - 49.5 kJ mol^{-1} for the complexes involving 2 DME and 2 TMA molecules, respectively. These values are slightly smaller than double the complexation energies of the 1:1 complexes reported in Table 1 (-39.7 kJ mol^{-1} and -50.6 kJ mol^{-1}), indicating a small anti-cooperative effect. The fact that this anti-cooperative effect is rather minute is consistent with the small charge transfer from the Lewis bases towards C_6F_6 observed in the previously mentioned NBO-analysis.

To demonstrate the stoichiometry of the complex present in the solutions, a concentration study [42] in which mixtures with different concentrations are measured at 120 K was performed. By plotting the integrated intensity of a complex band against the product of integrated intensities of the monomers, for different ratios of the monomers, the stoichiometry of the complex can be determined. The general principles and results of these concentration studies are given in Figures S7 and S8 of the ESI. The

data clearly show that for both Lewis bases a linear correlation is found only for a proposed 1:1 stoichiometry, which supports the idea that in the solutions mainly 1:1 complexes are formed.The appearance of weak spectral features red shifted from the 999.0 cm^{-1} monomer transition and from the 997.8 cm^{-1} and 996.5 cm^{-1} transitions assigned to the 1:1 complexes with DME and TMA respectively, also indicates the formation of 1:2 complex, albeit with an equilibrium concentration substantially smaller than that for the 1:1 complex. As an example, the spectra of the complex bands of C_6F_6.TMA mixtures with different TMA concentrations, as well as their differential spectrum, is given in Figure S9. Further indication that 1:2 complex is only present in a small amount compared to the 1:1 complex is supported by the fact that the gradients of the Van 't Hoff plots are not influenced by omitting the measurements at the lowest temperatures. We have therefore retained the results of the lowest temperatures in the construction of the Van 't Hoff plot, even though these are most likely to contain some intensity of the 1:2 complex.

Conclusions:

The existence of an attractive interaction between C_6F_6 and the Lewis bases DME(-d_6) and TMA(-d_9) has been demonstrated experimentally through the use of FTIR on LKr solutions. By comparing experimental complexation shifts with shifts obtained from *ab initio* calculations, it was found that the 1:1 complexes are formed through lone pair$\cdots\pi$ type interactions. Furthermore, indications for the presence of a small amount of 1:2 complex, involving 2 Lewis base molecules on opposite sides of the C_6F_6 molecular plane were found for mixtures with both DME(-d_6) and TMA(-d_9). For the complex with DME, a complex geometry with C_s symmetry was calculated in which the methyl groups of DME are tilted towards C_6F_6, enabling the formation of secondary interactions, which have been visualized using NCIPlot. For the interaction with TMA, a complex with C_{3v} geometry was obtained, in which the methyl groups of TMA are eclipsed with the carbon atoms of C_6F_6. From the construction of Van 't Hoff plots, experimental complexation enthalpies of –6.0(6) kJ mol^{-1} and –6.7(9) kJ mol^{-1} were determined for the 1:1 complexes involving DME(-d_6) and TMA(-d_9), respectively.

Supporting Information Available:

MP2/aug-cc-pVDZ cartesian coordinates, vibrational frequencies and IR intensities of all monomers and complexes, experimental frequencies of C_6F_6, DME-d_6 and TMA-d_9 and observed complex bands in LKr, ESP of benzene and hexafluorobenzene, NCI plots for both lp$\cdots\pi$ complexes, IR spectra of the regions of interest for C_6F_6 and mixtures involving DME-d_6 and TMA-d_9, typical Van 't Hoff plots for the lp$\cdots\pi$ complexes, the results from concentration studies for $C_6F_6\cdot$DME and $C_6F_6\cdot$TMA complexes and spectra of the $C_6F_6\cdot$TMA ν_{13} complex band for different TMA concentrations. This material is available free of charge via www.sciencedirect.com.

References:

1 J. S. Murray, P. Lane, T. Clark, K. E. Riley, P. Politzer, *J. Mol. Model.*, 2012, ***18***, 541-548.
2 G. Berger, J. Soubhye, A. van der Lee, C. Vande Velde, R. Wintjens, P. Dubois, S. Clément, F. Meyer, *ChemPlusChem*, 2014, ***79***, 552-558.
3 J. Ran, P. Hobza, *J. Chem. Theory Comput.*, 2009, ***5***, 1180-1185.
4 T. Korenaga, T. Shoji, K. Onoue, T. Sakai, *Chem. Commun.*, 2009, 4678-4680.
5 T. J. Mooibroek, P. Gamez, J. Reedijk, *CrystEngComm*, 2008, ***10***, 1501-1515.
6 A. Bauzá, T. J. Mooibroek, A. Frontera, *ChemPhysChem*, 2015, ***16***, 2496-2517.
7 M. Raimondi, G. Calderoni, A. Famulari, L. Raimondi, F. Cozzi, *J. Phys. Chem. A.*, 2003, ***107***, 772-774.
8 K. Pluhackova, P. Jurecka, P. Hobza, *Phys. Chem. Chem. Phys.*, 2007, ***9***, 755-760.
9 Y. Danten, T. Tassaing, M. Besnard, *J. Phys. Chem. A.*, 1999, ***103***, 3530-3534.
10 J. C. Amicangelo, D. G. Irwin, C. J. Lee, N. C. Romano, N. L. Saxton, *J. Phys. Chem. A.*, 2013, ***117***, 1336-1350.
11 C. J. Wormald, B. Wurzberger, *Phys. Chem. Chem. Phys.*, 2000, ***2***, 5133-5137.
12 M. Besnard, Y. Danten, T. Tassaing, *J. Chem. Phys.*, 2000, ***113***, 3741-3748.
13 M. Allesch, E. Schwegler, G. Galli, *J. Phys. Chem. B*, 2007, ***111***, 1081-1089.
14 P. Metrangolo, G. Resnati, T. Pilati, S. Biella, *Struct. Bond.*, 2008, ***126***, 105-136.
15 R. W. Troff, T. Mäkelä, F. Topić, A. Valkonen, K. Raatikainen, K. Rissanen, *Eur. J. Org. Chem.*, 2013, ***2013***, 1617-1637.
16 Y. Geboes, N. Nagels, B. Pinter, F. De Proft, W. A. Herrebout, *J. Phys. Chem. A*, 2015, ***119***, 2502–2516.
17 Y. Geboes, F. De Proft, W. A. Herrebout, *J. Phys. Chem. A*, 2015, ***119***, 5597-5606.
18 Q. Gou, G. Feng, L. Evangelisti, W. Caminati, *Angew. Chem. Int. Ed.*, 2013, ***52***, 11888-11891.
19 Q. Gou, L. Spada, Y. Geboes, W. A. Herrebout, S. Melandri, W. Caminati, *Phys. Chem. Chem. Phys.*, 2015, ***17***, 7694-7698.
20 I. Alkorta, I. Rozas, J. Elguero, *J. Org. Chem.*, 1997, ***62***, 4687-4691.
21 J. C. Amicangelo, B. W. Gung, D. G. Irwin, N. C. Romano, *Phys. Chem. Chem. Phys.*, 2008, ***10***, 2695-2705.
22 I. Alkorta, I. Rozas, M. L. Jimeno, J. Elguero, *Struct. Chem.*, 2001, ***12***, 459-464.
23 B. J. van der Veken, *J. Phys. Chem.*, 1996, ***100***, 17436-17438.
24 G. Herzberg, *Infrared and Raman Spectra of Polyatomic Molecules*, 12th ed., D. Van Nostrand Company Inc., Princeton, New Jersey, **1945**.
25 T. Shimanouchi, *Tables of Molecular Vibrational Frequencies Consolidated Volume I, Vol. 39*, Nat. Stand. Ref. Data Ser., Nat. Bur. Stand., Washington, D.C., **1972**.
26 M. J. Frisch, G. W. Trucks, H. B. Schlegel, G. E. Scuseria, M. A. Robb, J. R. Cheeseman, G. Scalmani, V. Barone, B. Mennucci, G. A. Petersson, H. Nakatsuji, M. Caricato, X. Li, H. P. Hratchian, A. F. Izmaylov, J. Bloino, G. Zheng, J. L. Sonnenberg, M. Hada, M. Ehara, K. Toyota, R. Fukuda, J. Hasegawa, M. Ishida, T. Nakajima, Y. Honda, O. Kitao, H. Nakai, T. Vreven, J. A. Montgomery, Jr., J. E. Peralta, F. Ogliaro, M. Bearpark, J. J. Heyd, E. Brothers, K. N. Kudin, V. N. Staroverov, R. Kobayashi, J. Normand, K. Raghavachari, A. Rendell, J. C. Burant, S. S. Iyengar, J. Tomasi, M. Cossi, N. Rega, N. J. Millam, M. Klene, J. E. Knox, J. B. Cross, V. Bakken, C. Adamo, J. Jaramillo, R. Gomperts, R. E. Stratmann, O. Yazyev, A. J. Austin, R. Cammi, C. Pomelli, J. W. Ochterski, R. L. Martin, K. Morokuma, V. G. Zakrzewski, G. A. Voth, P. Salvador, J. J. Dannenberg, S. Dapprich, A. D. Daniels, Ö. Farkas, J. B. Foresman, J. V. Ortiz, J. Cioslowski, D. J. Fox, *Gaussian 09, Revision D.01*, Wallingford CT, 2009.
27 S. F. Boys, F. Bernardi, *Mol. Phys.*, 1970, ***19***, 553-566.
28 H.-J. Werner, P. J. Knowles, G. Knizia, F. R. Manby, M. Schütz, P. Celani, T. Korona, R. Lindh, A. Mitrushenkov, G. Rauhut, K. R. Shamasundar, T. B. Adler, R. D. Amos, A. Bernhardsson, A. Berning, D. L. Cooper, M. J. O. Deegan, A. J. Dobbyn, F. Eckert, E. Goll, C. Hampel, A. Hesselmann, G. Hetzer, T. Hrenar, G. Jansen, C. Köppl, Y. Liu, A. W. Lloyd, R. A. Mata, A. J. May, S. J. McNicholas, W. Meyer, M. E. Mura, A. Nicklass, D. O'Neill, P.

Palmieri, D. Peng, K. Pflüger, R. Pitzer, M. Reiher, T. Shiozaki, H. Stoll, A. J. Stone, R. Tarroni, T. Thorsteinsson, M. Wang, *MOLPRO, version 2012.1, A Package of Ab Initio Programs*, 2012.
29 D. G. Truhlar, *Chem. Phys. Lett.*, 1998, ***294***, 45-48.
30 P. Jurecka, P. Hobza, *J. Am. Chem. Soc.*, 2003, ***125***, 15608-15613.
31 W. L. Jorgensen, *BOSS - Biochemical and Organic Simulation System*, John Wiley & Sons Ltd., New York, **1998**.
32 W. A. Herrebout, *Top. Curr. Chem.*, 2015, ***358***, 79-154.
33 E. R. Johnson, S. Keinan, P. Mori-Sánchez, J. Contreras-García, A. J. Cohen, W. T. Yang, *J. Am. Chem. Soc.*, 2010, ***132***, 6498-6506.
34 J. Contreras-García, E. R. Johnson, S. Keinan, R. Chaudret, J. P. Piquemal, D. N. Beratan, W. Yang, *J. Chem. Theory Comput.*, 2011, ***7***, 625-632.
35 D. Hauchecorne, R. Szostak, W. A. Herrebout, B. J. van der Veken, *ChemPhysChem*, 2009, ***10***, 2105-2115.
36 D. Hauchecorne, B. J. van der Veken, A. Moiana, W. A. Herrebout, *Chem. Phys.*, 2010, ***374***, 30-36.
37 N. Nagels, Y. Geboes, B. Pinter, F. De Proft, W. A. Herrebout, *Chem. - Eur. J.*, 2014, ***20***, 8433-8443.
38 J. H. S. Green, D. J. Harrison, *J. Chem. Thermodyn.*, 1976, ***8***, 529-544.
39 P. B. Davies, G. M. Hansford, T. C. Killian, *J. Mol. Spectrosc.*, 1994, ***163***, 138-158.
40 N. Nagels, D. Hauchecorne, W. A. Herrebout, *Molecules*, 2013, ***18***, 6829-6851.
41 B. Michielsen, J. J. J. Dom, B. J. van der Veken, S. Hesse, Z. Xue, M. A. Suhm, W. A. Herrebout, *Phys. Chem. Chem. Phys.*, 2010, ***12***, 14034-14044.
42 J. J. J. Dom, B. Michielsen, B. U. W. Maes, W. A. Herrebout, B. J. van der Veken, *Chem. Phys. Lett.*, 2009, ***469***, 85-89.

Graphical Abstract:

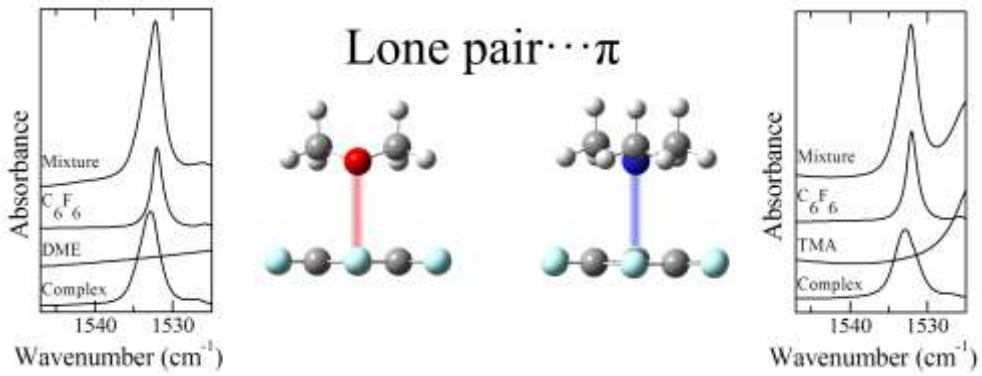

Bullet Points:

1) Cryosolutions of C_6F_6 with dimethyl ether or trimethylamine are studied with FTIR.
2) Complex bands are assigned to lone pair···π complex using *ab initio* calculations.
3) Assignment of observed monomer and complex bands is given.
4) Using Van 't Hoff plots, complex enthalpies of both complexes are determined.